NANO LETTERS

2007
Vol. 7, No. 6
1686−1691

Nanosize and Vitality: TiO_2 Nanotube Diameter Directs Cell Fate

Jung Park,[†] Sebastian Bauer,[‡] Klaus von der Mark,[†] and Patrik Schmuki*,[‡]

Department of Experimental Medicine I, Nikolaus Fiebiger-Center of Molecular Medicine, Germany, and Department of Materials Science, Friedrich-Alexander-University of Erlangen-Nuremberg, Germany

Received March 22, 2007; Revised Manuscript Received April 20, 2007

ABSTRACT

We generated, on titanium surfaces, self-assembled layers of vertically oriented TiO_2 nanotubes with defined diameters between 15 and 100 nm and show that adhesion, spreading, growth, and differentiation of mesenchymal stem cells are critically dependent on the tube diameter. A spacing less than 30 nm with a maximum at 15 nm provided an effective length scale for accelerated integrin clustering/focal contact formation and strongly enhances cellular activities compared to smooth TiO_2 surfaces. Cell adhesion and spreading were severely impaired on nanotube layers with a tube diameter larger than 50 nm, resulting in dramatically reduced cellular activity and a high extent of programmed cell death. Thus, on a TiO_2 nanotube surface, a lateral spacing geometry with openings of 30–50 nm represents a critical borderline for cell fate.

In the field of biomimetic materials and tissue implant technology, the importance of nanometric scale surface topography and roughness of biomaterials is, besides chemical surface modifications, increasingly becoming recognized as a crucial factor for tissue acceptance and cell survival.[1−3] Previous studies have indicated sensitivity of cellular responses to surface topography at a nanometric scale using nanoscale surface protrusions based on polymer demixing,[4] ordered gold cluster arrays,[5] or islands of adhesive ligands[6] at distinct length scales. Major achievements in the generation of geometrically defined, adhesive, and stable surfaces were made with the fabrication of self-organizing nanoporous Al and Si surfaces. Evidence is accumulating that lateral spacing of adhesive structures less than 100 nm may be superior in promoting cell adhesion on alumina nanosize particles.[7]

Recently, reports on the synthesis of TiO_2 nanotubes with various methods have generated considerable scientific interest owing to the broad range of applications of TiO_2.[8] A particularly attractive method for the production of TiO_2 nanotubes is the controlled anodization of Ti or Ti-based biomedical alloys in a fluoride-containing electrolyte as self-organized and highly ordered layers of nanotubes.[9−11]

Here we report on the cell response to this highly defined spacing variation that is vertically aligned TiO_2 nanotubes with six different diameters between 15 and 100 nm. Generation of self-assembled TiO_2 nanotubes in a highly regular arrangement was achieved by anodizing Ti sheets in a phosphate−fluoride electrolyte at different voltages ranging from 1 to 20 V, thus precisely controlling tube diameter[11,12] (Figure 1). In analyzing adhesion and growth of mesenchymal stem cells on these nanotubes (Figure 2), we show that on the nanotube layer cell fate is determined by a much smaller scale microenvironment than expected. A maximum stimulated cell response was elicited at a lateral spacing of 15−30 nm, which corresponds approximately to the predicted lateral spacing of integrin receptors in focal contacts on the extracellular matrix.[13] Cell adhesion, spreading, and growth on surfaces of this nanometric scale was enhanced in comparison to plain TiO_2 surfaces, while cells hardly attached and grew, but underwent apoptosis on 100 nm nanotubes (Figure 2E)

To investigate the cellular behavior in response to pore size, green fluorescent protein (GFP)-labeled rat mesenchymal stem cells were seeded on TiO_2 nanotube layers with six different diameters between 15, 20, 30, 50, 70, and 100 nm (Figure 1) as well as on smooth, polished TiO_2 layers for control. Cell adhesion and spreading was highest on 15 nm tubes and declined significantly with increasing pore size (Figure 2A). Analyzing adherent cells by fluorescence microscopy and scanning electron microscopy (SEM) revealed that cells spread out normally on smaller size nanotubes (15−30 nm), forming lamellopodia and wide, thick filopodia comparable to smooth surfaces. In contrast, on 100 nm nanotubes, cell adhesion and spreading was impaired without stable extension of filopodia after 24 h, while abundant thin microvilli were detectable both by

* Corresponding author. E-mail: schmuki@ww.uni-erlangen.de. Patrik Schmuki, Prof. Dr., Department of Materials Science, WW4-LKO, University of Erlangen-Nuremberg, Martensstrasse 7, D-91058 Erlangen, Germany. Telephone: +49-9131-8527575.

[†] Department of Molecular Medicine I, Nikolaus Fiebiger-Center of Molecular Medicine.

[‡] Department of Materials Science.

10.1021/nl070678d CCC: $37.00
Published on Web 05/16/2007

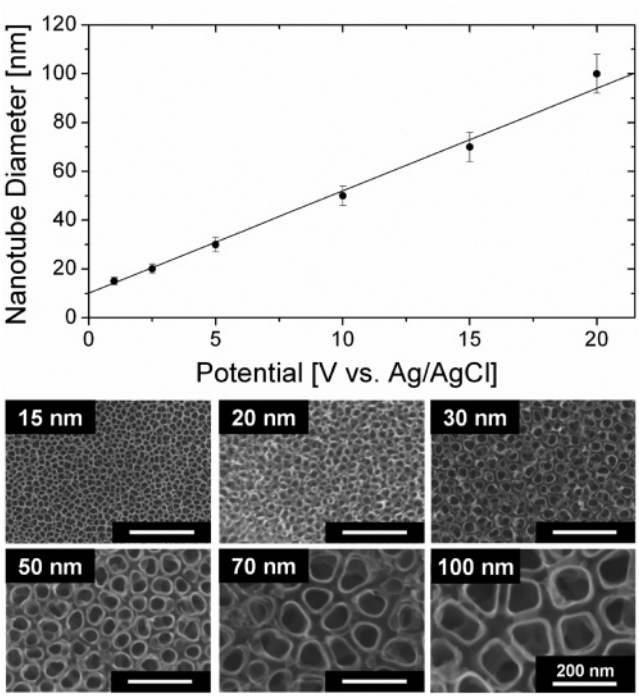

Figure 1. Surface of layers of self-aligned TiO_2 nanotubes with different diameters. Self-assembled layers of vertically oriented TiO_2 nanotubes were generated by anodizing titanium sheets. SEM images show highly ordered nanotubes of six different pore sizes between 15 and 100 nm created by controlling potentials ranging from 1 to 20 V.

fluorescence microscopy and by SEM. The cytoplasm was frequently perforated with disrupted cell contacts to the surface (see Supporting Information Figures S1 and S2).

The critical size of 15−30 nm for eliciting stimulated cellular responses became most apparent by analyzing the formation of focal contacts using paxillin as a marker protein. While cells grown on 30 nm and smaller diameter nanotubes showed extensive formation of paxillin-positive focal contacts to which actin stress fibers were anchored (Figure 3Aa,c), cells did not spread well on 100 nm tubes but developed a highly migratory morphology with long protrusions (Figure 3Ab,d) and only a few focal adhesions. Immunogold labeling of adherent cells with antibodies against paxillin and β1 integrin and examination by SEM revealed clustering of paxillin in focal contacts on 15 nm tubes but very few particles on the 100 nm surface (Figure 3B). On that surface, cells did not spread but sent out repeatedly cell protrusions that quickly retracted as visualized by video microscopy (see Supporting Information Figure S3 and videos), indicating that adherent mesenchymal cells react very fast and sensitive to the 100 nm diameter nanoscale openings. This finding supports recent reports on cells reacting sensitively to nanoscale roughness on silicon or silica substrates.[14,15] The high extent of focal contact formation seen on nanotubes smaller than 30 nm indicated activation of integrin-mediated signaling pathways controlling cell proliferation, migration, differentiation, and cell survival.

Cell proliferation rates, as measured by counting cells after 3 days and by a colorimetric assay (WST assay), were highest on the 15 nm diameter nanotubes, exceeding even proliferation rates on smooth polished surfaces (Figure 2B,C). Proliferation rates were decreasing with increasing tube diameter and lowest on 100 nm nanotubes. Similarly, cell motility measured in a wounding assay for 36 h was high on nanotubes smaller than 30 nm diameter but impaired on 100 nm nanotubes (Figure 2D).

Cell differentiation of mesenchymal stem cells into osteogenic lineages as determined by analyzing mineralization with alizarin red (Figure 2F) and osteocalcin immunofluorescence (Figure 3D) was also highest on 15 nm tubes but severely impaired on 100 nm sized nanotubes. Most remarkable was the strong induction of apoptosis on 100 nm tubes, as seen by surface labeling with FITC-labeled annexin V and TUNEL analysis in more than half of the cells within 48 h, continuing during days 3 and 4 (Figures 2E, 3D).

Cell interactions with extracellular surfaces, mostly the extracellular matrix and other cells, are mediated by integrins that control all major cellular activities including adhesion, changes in cell shape, proliferation, migration, differentiation, gene expression, and apoptosis in a synergistic manner with hormones and growth factors[16,17] Cell adhesion to the extracellular matrix causes clustering of integrins into focal adhesion complexes and activation of intracellular signaling cascades into the nucleus and to the cytoskeleton.[18,19] Functional focal adhesion complexes grow in size and complexity with time of adhesion and recruit numerous proteins such as FAK, vinculin, paxillin, tensin, c-src, p130Cas, and others.[18,20] In fact, phosphorylation of focal adhesion kinase FAK and the ERK kinase, which is a target of the FAK signaling pathway, was highest in stem cells growing on 15 nm nanotubes but low on 100 nm nanotubes (Figure 3C). Critical for integrin clustering and activation are concentration and topography of cell adhesion sites in the extracellular matrix.

The present results indicate that a spacing of 15 nm provides the optimum length scale for integrin clustering and focal contact formation, inducing cell proliferation, migration, and differentiation at a higher rate than on polished TiO_2 surfaces. The predicted size of surface occupancy by the head of an integrin heterodimer consisting of a β-propeller of the α-chain and the A domain of the β-chain is about 10 nm in diameter as estimated from electronmicrographic imaging of individual integrin molecules.[13] This suggests that a 15−20 nm spacing will allow or force clustering of integrins into the nearly closest packing possible, resulting in optimal integrin activation. Tube diameters larger than 50 nm, however, severely impaired cell spreading, adhesion, and spacing of 100 nm almost completely prevented integrin clustering and the formation of focal adhesion complexes, resulting in dramatically reduced cell proliferation, migration, and differentiation, and finally in the induction of anoikis, which is the adhesion-dependent form of apoptosis.

The critical spacing dimensions defined in this study are in line with a study on RGDfK-coated cell-adhesive gold nanodots spotted in distinct spacings of 28, 58, 73, and 85 nm distance, using block-copolymer micelle nanolithography.[2,21] In this study, a separation of >73 nm between dots

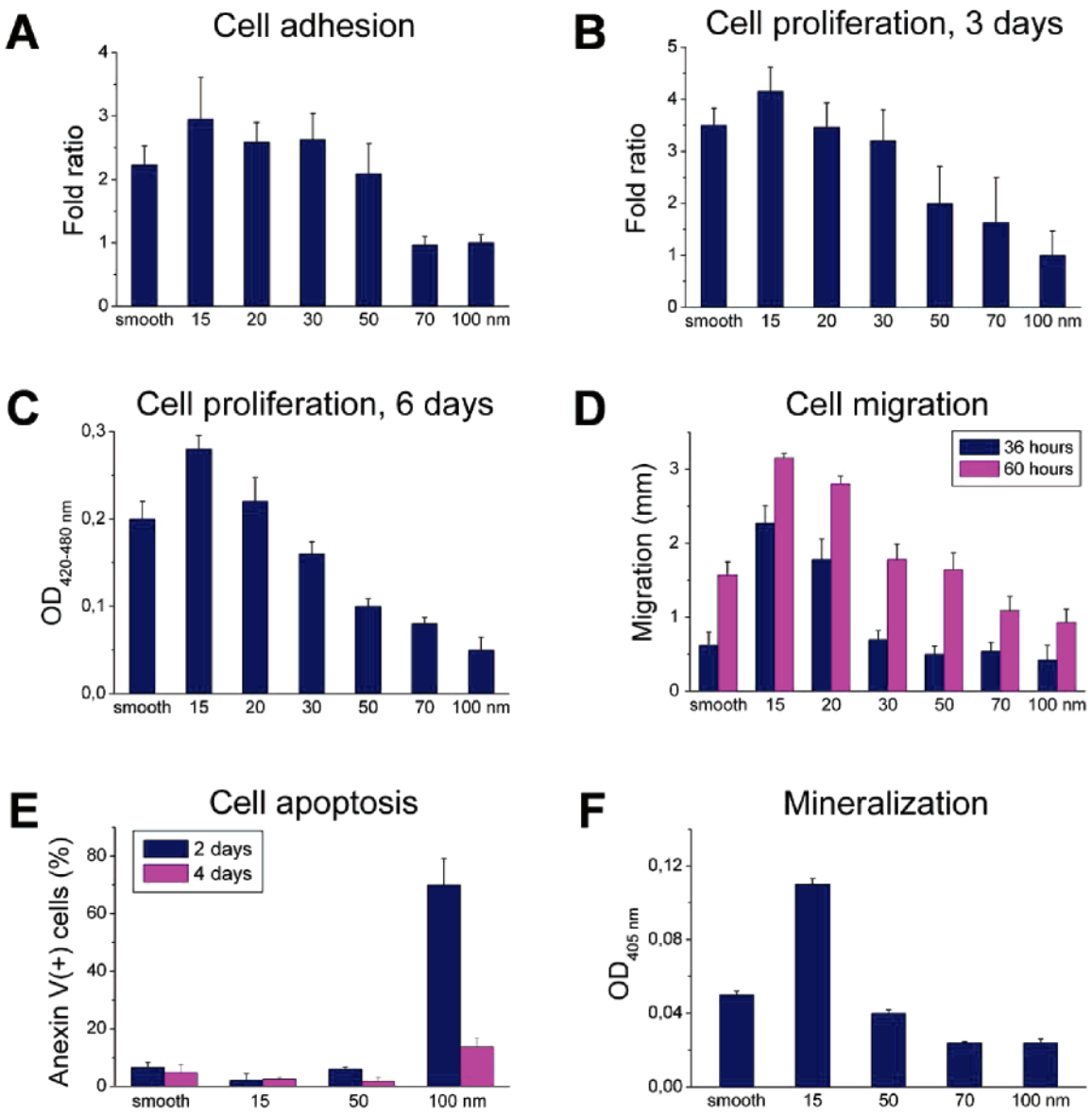

Figure 2. Cellular responses to nanoscale spacing distances. GFP-labeled rat mesenchymal stem cells were plated in culture medium containing 2% fetal calf serum on titanium chips coated with TiO_2 nanotubes of six different diameters; polished TiO_2-coated chips served as control ("smooth"). (A) For measuring cell adhesion, samples were washed 1 h after cell plating, and adherent cells were counted under the fluorescence microscope. Cell proliferation rates were measured by counting adherent cells after 3 days (B) and by a colorimetric WST assay 6 days after cell plating (C). (D) For measuring cell migration in a wounding assay, cells were plated at a density of 50 000 cells/cm^2, and 3 h later, a track of 3.4 mm width was created in the confluent cell layer. Cell motility was evaluated by measuring the remaining width after 36 and 60 h. (E) Apoptosis was analyzed by staining cells with Annexin V-FITC 2 and 4 days after plating (cell density of 5000/cm^2). Surface-labeled cells were counted using a fluorescence-activated cell sorter. (F) Osteogenic differentiation of stem cells after 2 weeks of cell culture in osteogenic differentiation medium was assessed by staining for calcium phosphate mineral deposition with alizarin red and colorimetric analysis of the dye.

resulted in limited cell attachment and spreading. In another study, osteoblast adhesion was enhanced by 50% on a porous alumina surface with less than 72 nm pore size as compared to amorphous alumina surfaces.[7] This may indicate that our findings are not limited to TiO_2 surfaces but address a universal cell response to topographic surface spacing. A key advantage of the TiO_2 nanotube model is that it is based on long-range self-assembly, i.e., large surface areas can uniformly be coated. Therefore, long-term investigations of cell behaviors such as proliferation, differentiation, and mineralization can easily be performed. Moreover, it combines the chemistry of a clinically relevant material used in contemporary biomedical implant devices with a self-organizing geometry that can be tuned over an unprecedented size range.

Our results, to the best of our knowledge, are the first report showing a dramatic change ranging from a strong stimulating effect of cell activities to a massive programmed cell death by controlling a nanotube surface geometry in a range of less than 100 nm. Because of the material selected, a "bio-inert" titanium oxide surface, our findings have an important impact on the design of implant surfaces and other biomaterials. A number of reports have shown that the surface structure of titanium is critical for determining the

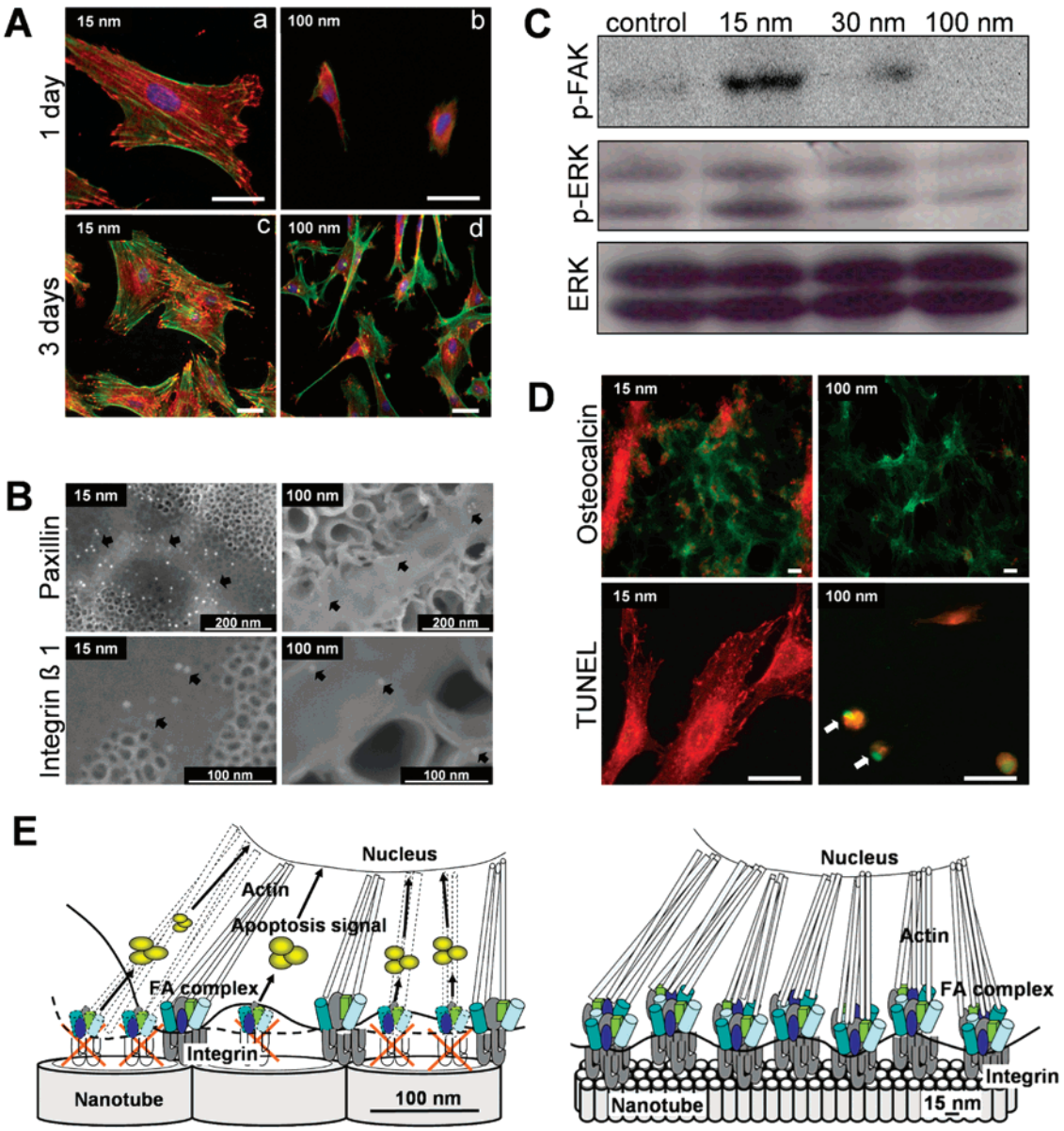

Figure 3. Focal contact formation, differentiation, and apoptosis of mesenchymal stem cells on 15 and 100 nm nanotubes. (A) On 1 and 3 days after plating, focal contact formation and stress fiber assembly was extensive on 15 nm nanotubes (a,c) as shown by anti paxillin staining (a,b,c,d, red) and anti-actin staining (green), but strongly reduced on 100 nm nanotubes (b,d). At 3 days, cells were well spread on 15 nm tubes (c), but developed a migratory morphology on 100 nm tubes with few focal contacts and stress fibers (d). Blue: DAPI for nuclear staining. Bars: a,b: 50 μm; c,d: 100 μm. (B) Analysis of focal contacts by SEM using immunogold staining with paxillin and β1-integrin antibodies revealed dense packing of paxillin in focal contacts on 15 nm tubes, while labeling was sparse on 100 nm tubes. (C) High extent of focal contact formation on nanotubes smaller than 30 nm as compared to 100 nm nanotubes, and a flat TiO_2 surface (control) was confirmed by analysis of phosphorylation of the foal adhesion kinase (FAK) and extracellular-regulated kinase (ERK) 1 h after cell plating. The Western Blot using whole cell lysates (10 μg/lane) with antibodies against phospho-FAK (Tyr526) and phospho-ERK proteins show a maximum of phosphorylation on 15 nm nanotubes. Antibody labeling of total ERK served as a loading control. Full length blots are presented in Supporting Information Figure 4. (D) Osteogenic differentiation occurred after 2 weeks in culture in osteoblast differentiation medium on 15 nm nanotubes as seen by osteocalcin staining (red, upper panels), but rarely detectable on 100 nm nanotubes. F-actin staining is in green. Bar, 20 μm. TUNEL staining (green, lower panels) showed extensive apoptosis on 100 nm tubes starting already 3 days after cell plating, but not on 15 nm nanotubes (see also Figure 2). Cells were counterstained for paxillin (red). Bars, 100 μm. (E) Nanoscale spacing directs cell fate: Hypothetical model showing the lateral spacing of focal contacts on nanotubes of different diameters. A spacing of 15 nm seems optimal for integrin assembly into focal contacts, thus inducing assembly of actin filaments and signaling to the nucleus. Nanotubes larger than 70 nm diameter do not support focal contact formation and cell signaling, thus leading to apoptosis (anoikis).

success or failure of clinical titanium implantations for the purpose of bone, joint, or tooth replacements. In the past, numerous studies on implant surface modifications have been performed at the micrometer scale to optimize the surface geometry and profile to best fit cell interactions for adequate bone growth.[22,24] Recently efforts have been made to improve cell stimulating, biomimetic activities by designing new surface geometries at nanoscale.[1,2,14,22] However, the present findings directly show that the sub-100 nm scale of microenvironments must be targeted as a scale of focus for the

biocompatibility of medical implant devices. Surface modification by nanotube layers may be particularly interesting because it allows not only to improve the mechanical properties and biocompatibility of the surface of medical implants by controlling the lateral spacing geometry, but also offers the opportunity to additionally regulate the cell fate by filling the nanotubes with biologically active signaling molecules. In conclusion, the use of TiO_2 nanotubes of controlled diameter may provide a powerful tool to improve cell adhesion and tissue integration of various cell types that may respond individually to different size nanotubes. Moreover, TiO_2 nanotubes can be designed to support cell functions of osteoblasts including differentiation and thus will turn out to be useful for coating of osteointegrative implant material.

Materials and Methods. *Nanotube Formation.* Titanium foils (99.6% purity, Advent Ltd.) were used for producing nanoporous surfaces. An electrochemical cell with a three-electrode configuration was used. A platinum gauze served as a counter electrode and a Haber−Luggin capillary with a Ag/AgCl (1 M KCl) electrode was used as a reference electrode. Electrochemical experiments were carried out with a high-voltage potentiostat (Jaissle IMP 88−200 PC). For nanoporous samples, 1 M H_3PO_4 (Merck) with addition of 0.3 wt % of HF (Merck) was used as electrolyte. Anodization was carried out with potentials from 1 V up to 20 V at room temperature. For smooth, polished surfaces, titanium sheets (99.99% purity, Alfa Aesar) were mechanically ground, lapped, and finally polished (New Lam System), followed by anodization in fluoride-free 1 M H_3PO_4 at 20 V. All electrolytes were prepared from reagent-grade chemicals and deionized water. After electrochemical treatment, the samples were rinsed with deionized water. For morphological characterization of sample surfaces, a field emission scanning electron microscope (S-4800, Hitachi) was used. Samples were cleaned with 70% ethanol solution and rinsed in phosphate-buffered saline (PBS) solution three times for 15 min before cell plating.

Cell Culture. Rat mesenchymal stem cells were isolated and expanded from fresh bone marrows from femurs of 4-week-old Wistar rat as described previously.[25] Selected clonal cells were further expanded in medium containing 60% DMEM-LG (Gibco BRL), 40% MCDB-201 (Sigma), and supplemented with 1× insulin−transferrin−selenium (Sigma), 1× linoleic acid−bovine serum albumin (Sigma), 10^{-9} M dexamethasone (Sigma), 10^{-4} M ascorbic acid 2-phosphate (Sigma), 100 units of penicillin, 1000 units of streptomycin (Gibco), 10 ng/mL EGF (Sigma), 10 ng/mL PDFG-BB (R&D Systems), and 1000 units/mL of rat LIF (Chemicon), and 2% fetal calf serum (FCS, Hyclone Laboratories). The expanded cells showed multipotent potential to differentiate into multiple mesenchymal lineages including osteoblast, chondroblast, adipocyte, myoblast, myofibroblast, and endothelial cells in differentiation experiments in vitro. For cell proliferation and migration assay, the cells were infected with retroviruses containing a green fluorescence protein (GFP) cDNA, and a stable GFP-expressing clone was used. For each experiment, cells were trypsinized and plated on each different size of nanotubes or smooth polished titanium surface at cell densities as indicated in DMEM: MCDB-201 medium mix as described above with 2% FCS without growth factors. For osteogenic differentiation, cells were plated at the cell density of 50 000/cm^2 in alpha medium (Invitrogen) containing 10% FCS. Five days after cell plating, culture medium was changed into differentiation medium containing 10% FCS, dexamethasone (100 nM), β-glycerophosphate (10 mM), and ascorbic acid (50 μg/mL). The cells were cultivated for 2 weeks and analyzed by immunocytochemistry and quantitative mineralization assay. The culture medium was replaced every 2 days in all experiment.

Protein Assay and Immunocytochemistry. For Western Blot analysis, cells were plated on 9 cm^2 titanium plates with a cell density of 50 000 /cm^2. One hour after cell plating, cells were washed twice with PBS and lysed in RIPA buffer supplemented with 1 mM sodium vanadate, 1 mM PMSF, 5 μg/mL leupeptin, and 5 μg/mL aprotinin at room temperature (RT) for 10 min. The lysates were cleared by centrifugation at 10 000*g* for 10 min at 4 °C. Supernatants (5 μg/lane) from total cell lysates were separated by 10% SDS-PAGE. Electroblotting onto nitrocellulose membrane and detection of proteins was performed with appropriate antibodies using the ECL detection system. The antibodies used were: rabbit polyclonal anti-phospho-FAK (Tyr526) (Cell Signaling), rabbit polyclonal anti-phospho-ERK (Cell Signaling), and rabbit polyclonal anti-ERK1 and ERK2 (Santa Cruz).

For immunocytochemistry, cells grown on nanotubes for 1 or 2 days after plating with a cell density of 5000/cm^2 were rinsed in PBS and fixed with 2% PFA in PBS at RT for 10 min. After fixation, cells were permeabilized with 0.2% Triton X-100 in PBS for 2 min, washed with PBS, and incubated with antibodies of mouse monoclonal anti-paxillin (Signal Transduction) and mouse monoclonal anti-osteocalcin (Takara) for 1 h. The F-actin was visualized with Alexa488-labeled phalloidin (Biosource). Secondary antibodies labeled with Cy5 (Biosource) were used. Cell nuclei were stained blue with DAPI (Roth). Cell images were taken using an Axiovert 2000 ApoTome microscope with an AxioCam digital camera and AxioVision software (Zeiss).

For immunogold stainings, 1 day after cell plating, cells were fixed with 2% PFA for 10 min and washed with PBS including 0.2 mM Glycin. Cells were permeabilized with 0.2% Triton X-100 in PBS for 2 min for anti-paxillin staining, then washed with PBS. The samples were blocked with bovine serum albumin and incubated with primary antibodies, mouse monoclonal anti-paxillin, or mouse monoclonal anti-integrin β1 (Invitrogen), for 1 h. After washing with PBS, the samples were incubated with 10 nm gold particle-conjugated anti-mouse IgG & M antibody diluted 1:30 in PBS for 1 h followed by washing with PBS the samples.

For SEM observation, cells were fixed with 2.5% glutaraldehyde solution (Merck) overnight at 4 °C. Samples were rinsed in PBS solution, dehydrated in a series of acetone (60, 70, 80, 90, and 100%) and critical point dried with a Critical Point Dryer (CPD 030, Balzers).

Cell Proliferation and Migration Assay. GFP-labeled mesenchymal stem cells were plated on titanium surface at a cell density of 5000/cm^2. For cell adhesion experiments 1 h after cell plating on 1 cm-diametered samples, non-adherent cells were washed out with PBS and adherent cells were counted at three different areas using 1280 × 1024 pixels resolution, each sample depicted under a fluorescent microscope (25× magnification). Cell proliferation was analyzed by a cell count 3 days after cell plating, or quantified at 6 days using the cell proliferation reagent WST-1 (Roche) according to the manufacturer's instructions. For a cell migration assay, GFP-labeled mesenchymal stem cells were plated at a cell density of 50 000/cm^2, and 3 h later, a 3.4 mm cleft was made in the center of titanium surface. Thirty-six h and 60 h later, the width of the remaining cleft was measured using Openlab software program (Improvision). At least three different areas were measured on 3 samples of each size of nanotube.

To analyze cell motility on different size of nanotubes, 1 day after cell plating, cell migration was monitored by time-lapse video microscopy every 2 min during 4 h and analyzed using Openlab software.

Apoptosis Assay. Cell apoptosis assays were performed by resuspending the cells 2 days and 4 days after plating on 9 cm^2 titanium plates with a cell density of 5000/cm^2 in 100 μL of binding buffer (10 mM HEPES, pH 7.4, 140 mM NaCl, 2.5 mM $CaCl_2$), followed by incubation with 5 μL of annexin V conjugated with FITC (a kind gift of Dr. Ernst Pöschl, Erlangen) for 15 min at room temperature in the dark. Propidium iodide was added immediately before analysis to exclude necrotic cells. Annexin V-positive cells were counted using a fluorescence-activated cell sorter. Additionally apoptotic cells were analyzed 2 days after cell plating by a TUNEL assay using a dead-end fluorescent TUNEL kit (Promega) according to manufacturer's instruction.

Acknowledgment. We gratefully appreciate the valuable help in the immunogold technique by Prof. Ursula Schloetzer-Schrehardt and Mrs. Rummelt, Eye Hospital, and Mrs. Friedrich for SEM investigations, Department of Materials Science, University of Erlangen-Nuremberg. This work was supported by the Deutsche Forschungsgemeinschaft (MA534/20-1 and SCHM1597/9-1).

Supporting Information Available: Adhesion and spreading of GFP-labeled rat mesenchymal stem cells on titanium sheets coated with 15 and 100 nm nanotubes. SEM of mesenchymal stem cells spread out 1 day after cell plating. Altered cell motility was shown on 100 nm nanotubes. Full scan blots depicted in Figure 3C. Cell motility on 100 nm nanotubes (Video 1) and 15 nm nanotubes (Video 2). Cell motility on different size of nanotubes 1 day after cell plating was observed by video microscope every 2 min during 4 h. This material is available free of charge via the Internet at http://pubs.acs.org.

References

(1) Craighead, H. G.; James, C. D.; Turner, A. M. P. *Curr. Opin. Solid State Mater. Sci.* **2001**, *5*, 177−184.
(2) Spatz, J. P. Cell-Nanostructure Interactions. In *Nanobiotechnology*; Wiley-VCH Verlag: Weinheim, Germany, 2004; pp 53−65.
(3) Wagner, V.; Dullaart, A.; Bock, A. K.; Zweck, A. *Nat. Biotechnol.* **2006**, *24*, 1211−1217.
(4) Dalby, M. J.; Riehle, M. O.; Yarwood, S. J.; Wilkinson, C. D.; Curtis, A. S. *Exp. Cell Res.* **2003**, *284*, 274−282.
(5) Boyen, H. G.; Kästle, G.; Weigl, F.; Koslowski, B.; Dietrich, C.; Ziemann, P.; Spatz, J. P.; Riethmüller, S.; Hartmann, C.; Möller, M.; Schmid, G.; Garnier, M. G.; Oelhafen, P. *Science* **2002**, *297*, 1533−1536.
(6) Cavalcanti-Adam, E. A.; Micoulet, A.; Blümmel, J.; Auernheimer, J.; Kessler, H.; Spatz, J. P. *Eur. J. Cell Biol.* **2006**, *85*, 219−224.
(7) Popat, K. C.; Chatvanichkul, K.-I.; Barnes, G. L.; Latempa, T. J., Jr.; Grimes, C. A.; Desai, T. A. *J. Biomed. Mater. Res. A* **2006**, *80*, 955−964.
(8) Macak, J. M.; Tsuchiya, H.; Taveira, L.; Aldabergerova, S.; Schmuki, P. *Angew. Chem., Int. Ed.* **2005**, *44*, 7463−7465.
(9) Zwilling, V.; Darque-Ceretti, E. *Electrochim. Acta* **1999**, *45*, 921−929.
(10) Macak, J. M.; Tsuchiya, H.; Schmuki, P. *Angew. Chem., Int. Ed.* **2005**, *44*, 2100−2102.
(11) Bauer, S.; Kleber, S.; Schmuki, P. *Electrochem. Commun.* **2006**, *8*, 1321−1325.
(12) Tsuchiya, H.; Macak, J. M.; Ghicov, A.; Schmuki, P. *Small* **2006**, *2*, 888−891.
(13) Takagi, J.; Petre, B. M.; Walz, T.; Springer, T. A. *Cell* **2002**, *110*, 599−511.
(14) Curtis, A. S. G.; Gadegaard, N.; Dalby, M. J.; Riehle, M. O.; Wilkinson, C. D. W.; Aitchison, G. *IEEE Trans Nanobioscience* **2004**, *3*, 61−65.
(15) Dalby, M. J.; McCloy, D.; Robertson, M.; Agheli, H.; Sutherland, D.; Affrossman, S.; Oreffo, R. O. C. *Biomaterials* **2006**, *27*, 2980−2987.
(16) Burridge, K.; Chrzanowska-Wodnicka, M. *Annu. Rev. Cell Dev. Biol.* **1996**, *12*, 463−518.
(17) Giancotti, F. G. *Dev. Cell* **2003**, *4*, 149−151.
(18) Schlaepfer, D. D.; Hauck, C. R.; Sieg, D. J. *Prog. Biophys. Mol. Biol.* **1999**, *71*, 435−478.
(19) DeMali, K. A.; Wennerberg, K.; Burridge, K. *Curr. Opin. Cell Biol.* **2003**, *15*, 572−582.
(20) Mitra, S. K.; Hanson, D. A.; Schlaepfer, D. D. *Nat. Rev. Mol. Cell Biol.* **2005**, *6*, 56−68.
(21) Arnold, M.;Cavalcanti-Adam, E. A.; Glass, R.; Blümmel, J.; Eck, W.; Kantlehner, M.; Kessler, H.; Spatz, J. P. *Chemphyschem* **2004**, *5*, 383−388.
(22) Schwartz, Z.; Boyan, B. D. *J. Cell. Biochem.* **1994**, *56*, 340−347.
(23) Zinger, O.; Anselme, K.; Denzer, A.; Habersetzer, P.; Wieland, M.; Jeanfils, J.; Hardouin, P.; Landolt, D. *Biomaterials* **2004**, *25*, 2695−2711.
(24) Bobyn, J. D.; Pilliar, R. M.; Cameron, H. U.; Weatherly, G. C. *Clin. Orthop. Relat. Res.* **1980**, *150*, 263−270.
(25) Jiang, Y.; Jahagirdar, B. N.; Reinhardt, R. L.; Schwartz, R. E.; Keene, C. D.; Ortiz-Gonzalez, X. R.; Reyes, M.; Lenvik, T.; Lund, T.; Blackstad, M.; Du, J.; Aldrich, S.; Lisberg, A.; Low, W. C.; Largaespada, D. A.; Verfaillie, C. M. *Nature* **2002**, *418*, 41−49

NL070678D